

# A study on the negative ion beam production in the ININ sputtering ion source

C. A. Valerio-Lizarraga, C. Duarte-Galvan, and I. Leon-Monzon  
*Facultad de Ciencias Físico-Matemáticas Universidad Autónoma de Sinaloa,  
 Avenida de las Américas y Boulevard Universitarios S/N, Sinaloa, 80010, Mexico.  
 e-mail: cvalerio@uas.edu.mx*

P. Villasenor and J. Aspiazu  
*Departamento de Aceleradores, Instituto Nacional de Investigaciones Nucleares,  
 Carretera México-Toluca S/N, Ocoyoacac, Estado de México, 52750, Mexico.*

Received 5 October 2018; accepted 10 January 2019

To improve the beam brightness produced in the 12 MeV Van de Graaff linear accelerator at Instituto Nacional de Investigaciones Nucleares we studied the beam generation inside the ion source. New 3D particle tracking simulations have been compared with measurements, and the agreement is better than using the traditional approach of only accounting for the primary beam. Among the results, it was observed that the main limit in the generation of intense beams is the suppression of the Cesium production due to space charge on the surface of the ionizers. In addition, the beam dynamics variation due to the erosion of the target inside the cathode has been determined. All these results allow us to find the optimal combinations for beam extraction.

*Keywords:* Accelerators; ion sources; plasma.

PACS: 29.25.Ni

## 1. Introduction

The Instituto Nacional de Investigaciones Nucleares (ININ) Tandem Van de Graaff accelerator provides different ion beams for fundamental research [1,2]. During its lifetime the machine has experienced several upgrades to improve the beam intensity, including the change of the ion source, and others main systems [3,4].

All these changes have left uncertainty in the evolution of the beam parameters (emittance, divergence, and brightness) along the Tandem, limiting the beam transmission to the experimental areas, and due to this uncertainty, it is complicated to assign the origins of the beam losses.

An intense beam dynamics study taking into account measurements and simulations needs to be performed to take advantage of all the machine capabilities using the new systems and mitigate the operation problems adequately [5], to finally achieve more precise measurements in the experimental areas.

As a first step, the research in this work will be focused on the ion source and low energy beam line, specially in the beam formation conditions with the aim of improve the overall machine performance.

## 2. Experimental Setup

The Source of Negative Ions by Cesium Sputtering source (SNICS) [6] is coupled to an electrostatic accelerator tube at 40 kV. A drift region connects this low energy acceleration stage to a 20° dipole magnet where the removal of electrons and the selection of the ion specie is achieved (see Fig. 1), then the Einzel lens focus the resulting beam, and it is monitored using a Faraday cup and a scintillator screen.

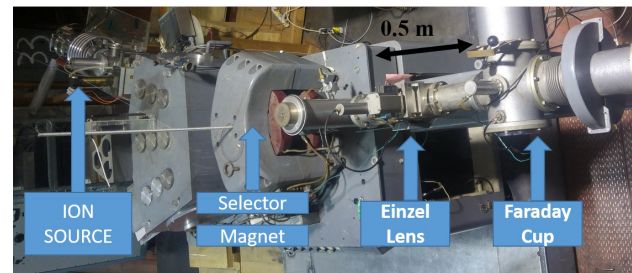


FIGURE 1. Low energy beam transport system including the 20° selector magnet.

In the acceleration stage, the accelerator tank reaches a maximum potential of 6 MV, and it is applied to a series of electrodes with a helical pattern for beam focus and acceleration. Half-way through the acceleration stage, the negative ions are stripped to positive ions by carbon films, with a target thickness of  $10 \mu\text{g}/\text{cm}^2$  allowing to reach a maximum energy of 12 MeV.

After the acceleration tank, a quadrupole system focuses the beam before it enters in the electromagnet (close to 1.0 T) where the ion energy is selected with a resolution in the order of KeV. Finally, the beam position is corrected before a horizontal dipole selects the beamline for the experiment.

### 2.1. Ion Source

Even though the production of negative ions is not well understood. It is used reliably to produce negative beams all around the world, and the SNICS ion source is an excellent example of it [7].

To produce the beam the SNICS uses Cesium (Cs) as a catalyst where the beam formation is driven by  $\text{Cs}^+$  sput-

tering a target inside a cathode holder. Regularly, the sputtered particles are neutral or positive, which pick up electrons while passing through a layer of Cs and produce negative ions. This technique can be used for different target materials, to generate the desired ion beam [8,9].

To create the appropriated Cs layer, a treatment of Cs vapors from an external heated Cs reservoir is applied with the aim of spread it into the cathode target and ionizer surfaces.

The ionizer is heated close to 1000°C (using a heating power between 125 and 135 W) and the neutral Cs in the ionizer surface is heated until been positively ionized. Then the Cs<sup>+</sup> ions are accelerated towards the cathode target due to a potential difference. In this process the ion source pressure is keep at 1 × 10<sup>-6</sup> mbar to control the negative beam neutralization.

Each charged particle generated in the target does need different conditions for the beam formation, the cathode-anode voltage is tunable to a maximum of 8 kV to find the best operation condition.

The target preparation also plays an essential role in the beam production, each time that the cathode holder is changed and set in place, the beam conditions change even when the beam to be generated is the same. This phenomenon will be investigated in later sections.

### 3. Simulation parameters

The Ion Beam Simulator (IBSIMU) [10] Y is a 3-D program used to simulate extraction systems and beam dynamics in the low energy beam transport systems. The simulations for this work take into account the electric field map generated by the electrodes potential distribution (Fig. 2) and the space charge produced by the charged particles traveling within the system, both contributions are combined solving the Vlasov equation (Eq. 1) by finite differences,

$$\vec{v} \cdot \nabla f - \frac{q}{m} (\vec{E} + \vec{v} \times \vec{B}) \cdot \frac{\partial f}{\partial \vec{v}} = 0, \quad (1)$$

where  $f(\vec{r}, \vec{v})$  is the particle distribution,  $E$  the electric field,  $v$  the particle velocity,  $m$  the mass and  $B$  the magnetic field.

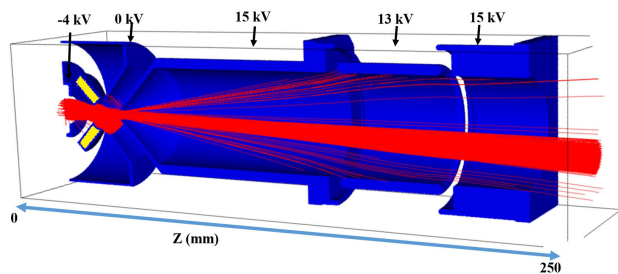


FIGURE 2. Extraction system and ion source simulation in IBSIMU including the beam (red), Cs ionizer (yellow), and electrodes (blue).

### 3.1. Extraction system and beam transport

A set of simulations were performed to study the maximum beam current transmission in the extraction system and beamline using the code TRAVEL [11] taking as input the ion source simulation output. The beam was tracked through the beamline including the 20° selector magnet up to the Faraday cup where a direct comparison between measurements and simulation was made (see Fig. 1).

The measurements and simulations suggest that not important ion beam losses (the electrons are lost in the magnet) had been observed once the focal elements are appropriately set. This allow us to be confident that the beam recorded at the Faraday cup will match the ion source transmission.

The simulations suggest that the beamline simplicity preserves the emittance but limits the control in the beam parameters at the entrance of the accelerator tank for an appropriated matching. Another important result from the simulations is that only for beam intensities close to 1 mA the beam space charge produce important beam losses.

## 4. Ion Source Simulations

The first ion source simulations were using a similar approach to other works [12]: an approximately Gaussian beam is generated in the target then it is tracked through the extraction system and beamline as Fig. 2 shows.

Using this simulation method for H<sup>-</sup> ions, the maximum beam width that can be extracted from the source is 180 μA, and for other ions like lithium it was 55 μA, where the anode aperture limits larger beam transmissions.

The previous results suggest that the beam space charge is not the source of the problem in the beam transport, because these beam intensities are well above the maximum obtained in the accelerator measurements.

Using maximum intensities from the measurements as input for the simulations, the behaviour is not the same. Once the anode cathode voltage is above 2 kV, we reach full transmission in disagreement with the measurements (Fig. 3).

After looking into the beam generation parameters without success, it was clear that this simulation method was not

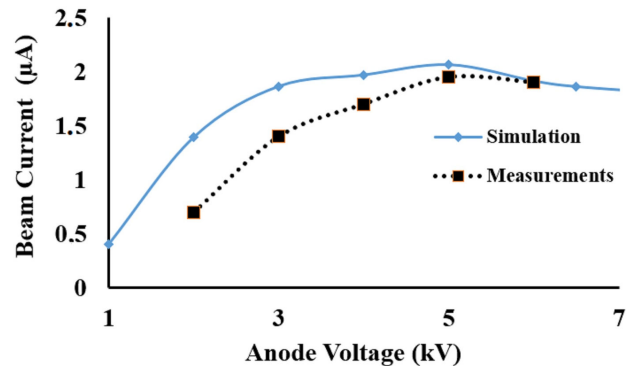


FIGURE 3. H<sup>-</sup> beam intensity recorded at the Faraday cup vs anode voltage.

good enough to reproduce the beam behavior in the ion source. Therefore, we decided to take a more realistic approach for the beam generation, by including the  $\text{Cs}^+$  beam generated by the ionizer.

## 5. Cs Ionizers geometries

In the ININ SNIC ion source, two ionizers have been used to generate negative beams; a Solenoidal Antenna Ionizer (SAI) [7] and a Conical Ionizer (CI) [13], both are heated by an external power source to produce the Cs. Due to the low beam intensity delivered by the source using the SAI, it was necessary to change it for the CI to produce more beam [14].

The origin of the low beam intensity in the SAI was never clear, reason why will be studied, even when it has been replaced.

To accurately model the ion source and implement the  $\text{Cs}^+$  ions generation in both ionizer geometries, the code IB-SIMU was modified to produce particles from curvilinear surfaces following the electrodes and ionizer curvature [15].

The new simulations also include the secondary electrons (not included in the figures for clarity) and ion production by the impact of the Cs ions into the surfaces [17]. The Fig. 4 shows the ionizer producing the  $\text{Cs}^+$  ions and the beam produced in the sputtering at the cathode surface, where the Cs beam trajectories depend on the voltage and geometry.

The current ratio yield  $J_{H^-}/J_{\text{Cs}^+}$  defines the negative beam emission from the cathode surface as the Cs ions collide, the accelerator operation shows a ratio close to 0.02 [16], and it will remain fixed for all this work.

Taking in to account the Faraday cup measurements and the yield ratio, with the cathode-anode voltage at 7 kV the ionizer produced up to 1 mA of  $\text{Cs}^+$  irradiation in to the cathode (the positive current recorded at the cathode electrodes confirms this  $\text{Cs}^+$  current). Also the sputtering production is simulated using the position of the Cs ions hitting the cathode as input.

In the next section, we study both geometries to find the operating limits and how to achieve higher intensities.

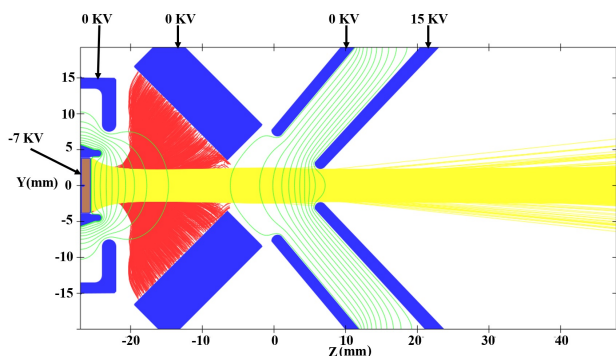


FIGURE 4. IBSIMU simulation of the SNIC ion source  $\text{Cs}^+$  (red), negative ion beam (yellow), and electrodes (blue).

### 5.1. Solenoidal Antenna Ionizers

During the ion source operation with the SAI, it produces uniform beams at intensities below  $1 \mu\text{A}$ , and experiences significant problems once we generate more  $\text{Cs}^+$  ions by increase the electric current running in the ionizer wires, where in some cases the negative beam intensity starts to decrease instead of increasing.

Due to the lack of tools to simulate and study such complex system, it was assumed that the irradiation on the SNICS surfaces produces a vacuum problem triggering the stripping losses.

The erosion pattern in the cathode used for beam production in high and low intensity shows some differences. The high-intensity beams end with a convex cathode surface and the ones used for the low-intensity end with a flatter surface using the same anode-cathode voltages giving a hint about the role of the Cs space charge.

Using the simulations we found that in the low intensity cases (less than 0.1 mA of  $\text{Cs}^+$ ) the anode-cathode voltage can be adjusted freely to achieve a uniform irradiation. The Fig. 5 shows the  $\text{Cs}^+$  generation by the SAI, as well as the irradiation profile at the cathode surface, setting the anode-cathode voltage to 7 kV.

The profile of the  $\text{Cs}^+$  irradiation shows a homogeneous irradiation on the cathode surface, suggesting that the final erosion will be homogeneous as in the experimental low intensity cases.

As the  $\text{Cs}^+$  current increases (above of 0.1 mA), the space charge plays an important role in the  $\text{Cs}^+$  emission and dynamics. The space charge screening of the electric potential in the back of the solenoid suppresses the emission, due to the SAI coils in the back are closer to the anode and the electric field is less intense.

Unfortunately the  $\text{Cs}^+$  ions produced in the coils at the back of the SAI are the ones hitting the cathode in the center, and once these coils stop its emission, only the closest to the cathode carry the irradiation, therefore a hollow irradiation is produced. These result explain why the cathode ends with a convex surface in the measurements.

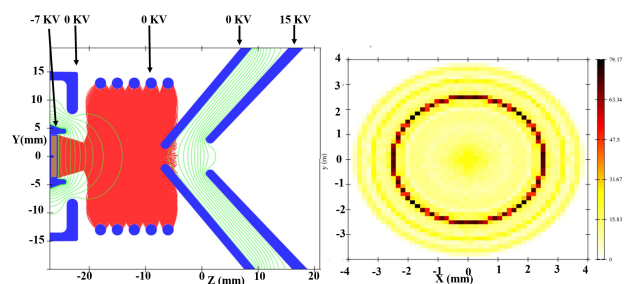


FIGURE 5. IBSIMU simulation of the SNIC SAI ionizer with  $\text{Cs}^+$  emission irradiating the cathode target (left), and the irradiation profile (right).

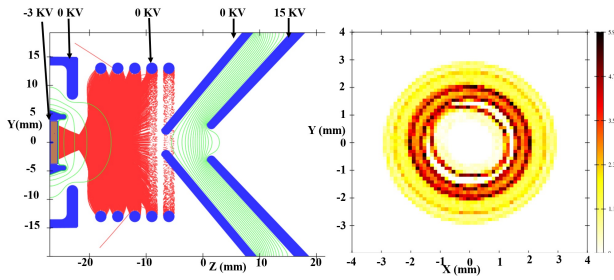


FIGURE 6. IBSIMU simulation: Suppression of the Cs<sup>+</sup> emission at the Solenoid ionizer surface due to space charge screening (left), and the irradiation profile at the cathode surface (right).

This hollow irradiation together with the small anode aperture (3 mm) produce a beam that can be stopped almost entirely in the anode electrodes and the SAI ends with less beam production even when the ionizer produces more ions.

The total space charge deposition (SCD) of all the ions involved in the simulation can be estimated with the Eq. 2 [16], where  $I_x$  the current from the particle  $x$ , assuming the electrons to Cs<sup>+</sup> ratio as one, the space charge is widely dominated by the Cs<sup>+</sup> ions by its mass and intensity and the inclusion of the electrons and ion beam does not change the Cs particles trajectories significantly as the simulations confirm.

$$SCD \propto I_{Cs^+} - \sqrt{\frac{m_{H^-}}{m_{Cs}}} I_{H^-} - \sqrt{\frac{m_e}{m_{Cs}}} I_e. \quad (2)$$

The previous results show that the longitudinal length of the SAI is not the optimum for the beam production. Using the same simulations it was found that by removing the closest turn to the cathode it is possible to extract more ions from the back of the antenna and achieve a centered irradiation. In consequence a new antenna with fewer turns is under design to avoid the screening problem in the high-intensity cases.

### 5.2. Conical Ionizer

The current ionizer used at the ININ ion source has a conical geometry, it also comes with a new configuration of the anode electrode where the aperture is twice as before. This change allows a higher transmission for bigger beam sizes, allowing the production of higher intensities than the previous ionizer configuration.

After the beam operation, the ionizer produces a concave surface at the cathode, indicating how the Cs<sup>+</sup> irradiation is more efficient using this geometry.

Previous works that use 2-D simulations [17,18] of this system have shown, they have shown, how the conical ionizer concentrates 90 % of the beam within a 2 mm spot in the cathode center with excellent uniformity. Figure 7 shows our 3-D simulations and confirms that the conical ionizer produces a more homogeneous irradiation on the cathode surface in comparison to the SAI, according to measurements (more than 95 % of the irradiation is within a spot of 2 mm).

The 3-D approach reveals how the irradiation peak at 7 kV is not in the cathode center, and instead it is allocated in

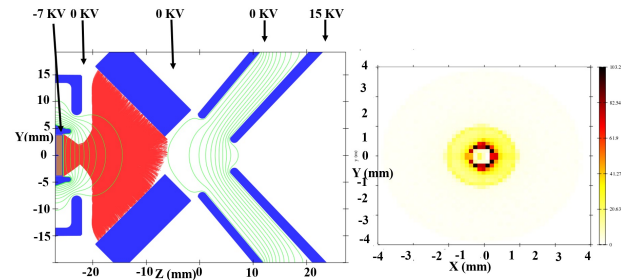


FIGURE 7. IBSIMU simulation: Conical Ionizer producing Cs beam (red) to irradiate the cathode (left) and the irradiation profile at the cathode surface (right).

a 0.4 mm circle due to Cs overfocusing, this result has profound implications for the beam intensity and quality [19], limiting also the maximum voltage to set.

To achieve an uniform target irradiation and eliminate the empty spot in the cathode center (Fig. 7), we change the Cs<sup>+</sup> current to improve the focal point, and this can be done to all the cathode-anode voltages.

Another unexpected deficiency revealed by the simulations, consist that in the back part of the cylinder, the anode-extractor voltage suppresses the Cs emission contributing to the hollow irradiation in the cathode, limiting the maximum extractor voltage. By decreasing the extractor voltage or by closing the anode electrode aperture this effect can be suppressed.

Measurements have shown how the Cs irradiation intensity at the cathode increases by 10 % if we decrease the extractor voltage from 10 kV to 7 kV with the anode-cathode voltage at 3 kV.

For the maximum beam transmission in to the Faraday cup, the beam has a halo component that covers all the beampipe. This halo is a product of the irradiation outside the 2 mm spot which is less than 5 % of the total beam. The measurements in the scintillator screen confirms the beam halo behavior, where as we decrease the anode-cathode voltage the beam halo disappears due to the beam collimation in the electrodes.

Comparing the new simulation approach to the measurements (Fig. 8), we have a better agreement that confirms that

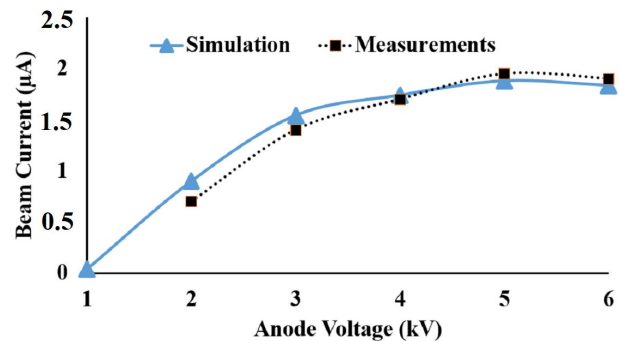


FIGURE 8. H<sup>-</sup> beam intensity recorded at the Faraday cup for measurements and simulations taking in to account the Cs ions to produce the beam.

it is necessary to take in to account the Cs<sup>+</sup> irradiation in the beam generation.

### 5.3. Target position

Using the conical ionizer we studied the role of the distance between the cathode and the ionizer in the beam generation. By design, it is suggested to place target surface sunken 2 mm in relation to the cathode holder, until now the effect of the target position and its impact in the beam dynamics for this source was not clear.

Typically, to maximize the cathode lifetime, this is filled to the top and due to the sputtering effect there is a continuous change in the location where the beam is generated (to deliver 2 μA of H<sup>-</sup> the cathode is consumed 0.5 mm per day).

In the Faraday cup the beam current decays as the cathode target is worn out, making it necessary to renew the targets to recover the beam intensity. In some cases, after a cathode renovation the current may fall below what the old cathode produced.

To simulate errors in the target preparation and the wear by sputtering, we changed the cathode target position getting a maximum H<sup>-</sup> transmission of 2.2 μA.

The Fig. 9 shows the correlation between the target position, anode voltage and transmission. Within ± 4 mm, it is possible to improve the beam transmission and emittance for the new cathode position by tuning the anode-cathode voltage. Once the target is sunken below 4 mm, the electric fields inside the cathode decay to levels where the beam production decays, and it is necessary to renew it.

The simulations and the Fig. 9 also suggest that it is necessary to tune the anode electrodes as the target sinks into the cathode holder, to properly focus the Cs<sup>+</sup> ions and the generated beam or the beam transmission will be affected.

For new targets, if it is sunken less than 1 mm into the holder edge (Fig. 10), the beam divergence increases, producing beam losses or even damages on the ionizer surface.

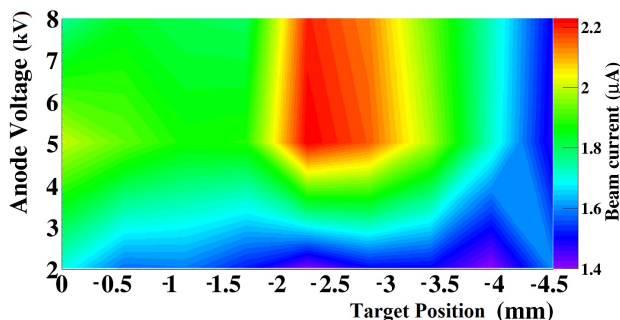


FIGURE 9. Negative Beam current recorded at the end of the extractor as function of the target position within the cathode container.

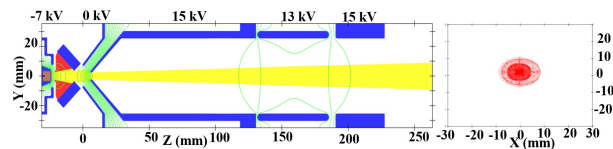


FIGURE 10. IBSIMU simulation: H<sup>-</sup> (yellow) and Cs<sup>+</sup> (red) trajectories (left) and beam profile at the end of the extraction system (right) for the Cathode target in line with the electrodes.

One positive aspect of the beam collimation on the electrodes is the beam emittance reduction at the end of the extraction system, obtaining 1 mm mrad emittance comparing to the 5 mm mrad for the source delivering the same current once the cathode is sunken 2 mm.

## 6. Conclusions

A comparison between measurements and 3-D simulations has been made in the SNICS source and transport to understand some operation problems towards the increase of the beam intensity.

The standard simulation method where a Gaussian beam distribution is used to generate the beam in the cathode surface, it is not good enough to reproduce the beam measurements.

A new simulation method has been implemented where the beam production depends on the Cs ions colliding on the target surfaces.

The changes in the Cs trajectories by the space charge and anode voltage impact on the beam formation in such a way that it reproduces the measurements adequately and explains some of the weak points in the source design.

The limit in the solenoidal ionizer to produce high-intensity beam arises from the Cs ions space charge that suppresses the emission in the most remote coils, which irradiate the cathode center in detriment of the emittance.

The conical ionizer irradiation is more uniform in comparison with the solenoidal antenna and the overfocusing of the Cs is the source of the beam halo that is seen in the beam-line measurements and simulation.

The extraction system can suppress the Cs production in the back part of the conical ionizer. One solution is to reduce the extraction voltage as we decrease the anode voltage.

For the target position inside the cathode holder, the simulations show how the cathode can be eroded up to 4 mm, and the beam transmission and emittance can be maintained. Also the continuous target erosion suggests that during operation it is necessary to tune the source to recover the beam quality without replacing the cathode.

1. J.C. Morales-Rivera, E. Martinez-Quiroz, T.L. Belyaeva, E.F. Aguilera, D. Lizcano, and P. Amador-Valenzuela, ().
2. J.C. Morales-Rivera, T.L. Belyaeva, P. Amador-Valenzuela, E.F. Aguilera, E. Martinez-Quiroz, and J.J. Kolata, ().
3. S. P. Villasenor *et al.*, in *XV ININ-SUTIN Technical and Scientific Congress* (Salazar, Mexico, 2004) pp. 1-6.
4. S. P. Villasenor, in *XVI ININ-SUTIN Technical and Scientific Congress* (Estado de Mexico, Mexico, 2006) pp. 6-7.
5. J. J. Ramirez *et al.*, in *XII ININ-SUTIN Technical and Scientific Congress* (Estado de Mexico, Mexico, 2002) pp. 4-6.
6. NEC SNICS cesium-sputter negative ion source, <http://www.pelletron.com/products/snics/>
7. G. T. Caskey, R. A. Douglass, H. T. Richards, and H. V. Smith, *Nuclear Instruments and Methods* **157** (1978) 1.
8. L. Escobar-Alarcon, D. A. Solis-Casados, F. Gonzalez-Zavala, S. Romero, M. Fernandez, and Haro-Poniatowski, *Journal of Physics: Conference Series* **792** (2017) 12006.
9. R. Policroniades, E. Martinez-Quiroz, B. Mendez-Garrido, G. Murillo, E. Moreno, and P. Villasenor, *AIP Conference Proceedings* **1671** (2015).
10. T. Kalvas *et al.*, *Rev. Sci. Instrum.* **81** (2010) 1.
11. J.-F. A. A.Perrin and T. Muetze.
12. B. X. Han, J. Southon, M. Roberts, and K. V. Reden, *Nuclear Instruments and Methods in Physics Research B* **261** (2007) 588.
13. J. Southon and G. M. Santos, *Nuclear Instruments and Methods in Physics Research B* **259** (2007) 88.
14. J. Flores, F. Aldape, R. V. Diaz, and D. Crumpton, *Nuclear Instruments and Methods in Physics Research* **75** (1993) 116.
15. K. L. Jensen, D. A. Shiffler, J. J. Petillo, Z. Pan, and J. W. Luginsland, *Phys. Rev. ST Accel. Beams* **17** (2014) 043402.
16. O. Midttun, J. Lettry, and R. Scrivens, *Review of Scientific Instruments* **85** (2014) 02A701.
17. J. H. Billen, *Nuclear Instruments and Methods in Physics Research* **220** (1984) 225.
18. O. Midttun, T. Kalvas, M. Kronberger, J. Lettry, H. Pereira, and R. Scrivens, *AIP Conf. Proc.* **1515** (2012) 481.
19. K. Devarani, in *Indian particle accelerator conference* (Kolkata, India, 2013) pp. 225-250.